**Journal of Physical Sciences: Theories, Methods and Applications**
Volume 1, Issue 1 (2026), pp. 27–46
ISSN: [print ISSN] (print), [online ISSN] (online)
https://jpstma.org
https://doi.org/10.68839/jpstma.2026.fvx2abgs
**Research article**

# Health-worker emigration and the loss of disease control: a coupled workforce-epidemic model with burnout-driven attrition

Timothy Ado Shamaki*

Department of Applied Mathematics, Federal University of Technology, Babura, Jigawa State, Nigeria

**Email address**
tashamaki.math@futb.edu.ng

**ABSTRACT**

Nigeria has lost a large share of its health workforce to emigration, and surveys of Nigerian health workers link the wish to emigrate with burnout. This paper couples a treatable infection of SIS type to a health workforce that is trained, practises and emigrates. Treatment capacity is proportional to the practising workforce, and the emigration rate of practising workers rises with disease prevalence, which stands for workload. The analysis gives four main results. First, the basic reproduction number depends on the workforce only through its disease-free level, which yields explicit critical values of the workforce, the baseline emigration rate and the training intake. Second, burnout-driven emigration alone can make the bifurcation at the threshold backward, even when treatment does not saturate; an explicit index decides the direction, and centre manifold theory confirms it. Third, without treatment saturation the fold point, the width of the hysteresis interval and the jump in prevalence are given in closed form, and each agrees with an independent numerical computation to at least ten significant digits. Fourth, when saturation is moderate, every solution converges to an equilibrium. Numerical continuation shows that once control is lost, reducing emigration back to the critical rate does not restore it. A global sensitivity analysis shows that burnout leaves the reproduction number unchanged but raises the long-run prevalence after a large outbreak. Allowing emigrants to return lowers both the reproduction number and the index. The parameter values are illustrative assumptions, not estimates for Nigeria, so the numerical thresholds show what the model can do rather than where any real health system stands.

**ARTICLE HISTORY**

**Received**
19 October 2026

**Accepted**
29 October 2026

**Published online**
30 October 2026

**CITE THIS ARTICLE**

T. A. Shamaki. Health-worker emigration and the loss of disease control: a coupled workforce-epidemic model with burnout-driven attrition. J. Phys. Sci., Theor. Methods Appl., 1(1), (2026), 27–46.

**Keywords:** Health-worker emigration, burnout, treatment capacity, backward bifurcation, hysteresis, global stability.

**Mathematics Subject Classification:** 92D30, 34C23, 34D23, 37N25.

## 1 Introduction

Many Nigerian doctors, nurses and midwives have emigrated in recent years, a movement known locally as "japa". The register of the UK Nursing and Midwifery Council shows how fast the movement has grown: the number of Nigeria-trained

*Corresponding Author: tashamaki.math@futb.edu.ng
© 2026 by the authors. Published by the Journal of Physical Sciences: Theories, Methods and Applications (JPSTMA). This article is an open access article distributed under the terms and conditions of the Creative Commons Attribution (CC BY) license (https://creativecommons.org/licenses/by/4.0/).

nurses and midwives on the register rose from 2,796 in March 2018 to 4,310 in March 2021 and to 7,256 in March 2022 [13]. In a survey of 913 physicians across 37 states, 43.9% wanted to emigrate [14], and about two-thirds of 763 early-career doctors in nine tertiary hospitals planned to do so [1]. The World Health Organization (WHO) reports 4.14 medical doctors per 10,000 population in Nigeria for 2024 [24]. For comparison, the WHO global strategy on human resources for health used an index of 4.45 physicians, nurses and midwives per 1,000 population, that is 44.5 per 10,000, to estimate workforce needs [22]. Nigeria is one of the 55 countries on the WHO health workforce support and safeguards list 2023 [21, 23].

Emigration and workload reinforce each other. Among 513 Nigerian health workers surveyed in 2023, 80.1% intended to emigrate, and the intention was associated with having experienced burnout [3]. Among 280 nurses in government hospitals in south-west Nigeria, 70.6% had job burnout and 89.3% had a strong intention to emigrate, and burnout mediated the link between working conditions and the intention to leave [2]. When workers leave, those who remain carry more patients. Disease burden is part of that workload, so an infection that the health system fails to control raises the pressure on the workforce, and the workforce that remains controls the infection less well. The epidemic and the workforce are therefore coupled in both directions.

Epidemic models with limited treatment describe one side of this coupling. Wang and Ruan [20] studied a constant removal rate of infectives and found Bogdanov–Takens, Hopf and homoclinic bifurcations. Wang [19] used a treatment rate that is proportional to the number of infectives up to a fixed capacity and showed that a low capacity produces a backward bifurcation. Zhang and Liu [25] replaced this piecewise rate by a saturated treatment function of the form $rI/(1+\alpha I)$, which also produces a backward bifurcation. Zhou and Fan [27] studied an SIR model with saturated treatment under limited medical resources and found Hopf and Bogdanov–Takens bifurcations, and Shan and Zhu [16] let the recovery rate depend on the number of hospital beds $b$ through $\mu_0 + (\mu_1 - \mu_0)\, b/(I+b)$, which produces backward, saddle-node, Hopf and Bogdanov–Takens bifurcations. Hsiao and Juang [10] added behavioural change to an SIS model with the capacity of Wang [19] and found degenerate Hopf and saddle-node bifurcations of limit cycles; they treat the maximum capacity as a parameter that a government can adjust.

In all of these models the capacity of the health system enters through fixed parameters: a removal rate, a capacity, a saturation constant or a number of beds. Their bifurcations arise because the treatment that each infected person receives falls as the number of infected people grows while the capacity stays fixed. In the present model the capacity is the practising workforce $H$, a state variable, and the treatment received per infected person falls for a second reason: a rising prevalence drives health workers to emigrate, so the workforce itself shrinks. This feedback can produce a backward bifurcation even when the treatment rate is proportional to the workforce and does not saturate. Section 3.9 makes the comparison precise, and Table 3 sets the treatment functions and the bifurcations of these models side by side. Models that include health workers usually treat them as a group at higher risk of infection, as in the study of SARS-CoV-2 among health-care workers by Gozalpour et al. [7]. I have not found a model in which the workforce that provides treatment is itself a state variable that grows by training and shrinks by emigration in response to the disease burden.

This paper builds and analyses such a model. A treatable SIS infection is coupled to three workforce compartments: trainees, practising health workers and emigrants. The treatment rate is proportional to the practising workforce, and the per-capita emigration rate rises linearly with prevalence. I prove five groups of results. First, the basic reproduction number depends on the workforce only through its disease-free level, which gives explicit critical values of the workforce, the baseline emigration rate and the training intake. Second, burnout-driven emigration can by itself make the bifurcation at the threshold backward; the direction is decided by an explicit index. Third, when treatment does not saturate, the fold point, the width of the hysteresis interval and the jump in prevalence at the threshold are explicit. Fourth, under a condition on the saturation constant, every solution converges to an equilibrium. Fifth, numerical continuation and a global sensitivity analysis illustrate these results. An extension in Section 3.8 lets emigrants return to practice. Each proof displays the intermediate steps, the direction of the bifurcation is confirmed independently by centre manifold theory, and every closed-form threshold is checked against an independent numerical computation.

The parameter values used in the simulations are assumptions chosen to illustrate the theorems. None of them was estimated from Nigerian data, so the numerical thresholds in Section 3 show what the model can do rather than where the Nigerian health system stands. Calibrating the model would require estimates of the baseline emigration rate $e_0$, the burnout sensitivity $\varepsilon$, the treatment rate per health worker $\kappa$ and the saturation constant $b$; Section 3.9 sets out the data that would provide them. Section 2 presents the model and the methods. Section 3 contains the analysis, an extension with return migration, the numerical results and a discussion. Section 4 concludes.

## 2 Materials and methods

### 2.1 Model formulation

I consider a population of constant size. Let $I(t)$, with $0 \le I(t) \le 1$, be the proportion of the population that is infected, so that $S = 1 - I$ is the susceptible proportion. The workforce is measured as a density per 10,000 population: $T(t)$ denotes trainees, $H(t)$ practising health workers who treat the infection, and $E(t)$ the cumulative number of health workers who have emigrated. The model rests on the following assumptions.

(A1) The infection confers no lasting immunity. Susceptible individuals are infected at rate $\beta SI$, and infected individuals clear the infection without treatment at rate $\gamma$.

(A2) Infected individuals are treated and cured at the per-capita rate $\kappa H/(1 + bI)$. The constant $\kappa$ is the treatment rate per unit density of health workers when the caseload is light, and $b \ge 0$ describes saturation: when $b > 0$, each infected person waits longer for treatment as prevalence rises. The case $b = 0$ means that treatment does not saturate.

(A3) Trainees enter at rate $\Lambda$, qualify at rate $\sigma$, leave training at rate $\mu_t$ and emigrate during training at rate $e_t$. Practising health workers leave the workforce for reasons unrelated to the infection (retirement, death or change of career) at rate $\mu_h$ and emigrate at the per-capita rate $e_0 + \varepsilon I$. The constant $e_0$ is the baseline emigration rate, and $\varepsilon \ge 0$ measures how strongly emigration responds to the disease burden, which I use as a proxy for workload and burnout.

(A4) Infection of health workers is neglected, and emigrants do not return, so the emigrated class $E$ in system (1) has no outflow. Section 3.8 relaxes the second assumption by letting emigrants return to practice.

Under these assumptions the model is

$$\begin{aligned}
\frac{dS}{dt} &= -\beta SI + \gamma I + \frac{\kappa HI}{1 + bI}, \\
\frac{dT}{dt} &= \Lambda - (\sigma + \mu_t + e_t)T, \\
\frac{dI}{dt} &= \beta I(1 - I) - \gamma I - \frac{\kappa HI}{1 + bI}, \\
\frac{dH}{dt} &= \sigma T - (\mu_h + e_0 + \varepsilon I)H, \\
\frac{dE}{dt} &= e_t T + (e_0 + \varepsilon I)H,
\end{aligned} \tag{1}$$

with non-negative initial values and $I(0) \le 1$. Figure 1 shows the flows. All parameters are positive except $b$ and $\varepsilon$, which are non-negative. The variable $E$ does not influence the other equations and only records the loss, so I omit it from the analysis of equilibria. I use the notation

The initial value of the susceptible proportion is $S(0) = 1 - I(0)$. Adding the first two equations of (1) gives $d(S + I)/dt = 0$, so $S(t) + I(t) = 1$ for all $t \ge 0$; this identity has been used to write $\beta SI = \beta I(1 - I)$ in the second equation. The equation for $S$ is therefore determined by the equation for $I$, and the analysis below works with $I$ alone. The susceptible class appears in Figure 1 because it is the class from which new infections are drawn.

$$k_t = \sigma + \mu_t + e_t, \quad T^* = \frac{\Lambda}{k_t}, \quad \pi = \sigma T^* = \frac{\sigma\Lambda}{k_t}, \quad m = \mu_h + e_0, \quad H_0 = \frac{\pi}{m},$$
$$I_{\max} = \max\left\{0, 1 - \frac{\gamma}{\beta}\right\}. \tag{2}$$

Here $\pi$ is the rate at which newly qualified workers join the practising workforce at equilibrium, $m$ is the exit rate of practising workers when there is no infection, $H_0$ is the disease-free workforce, and $I_{\max}$ is the equilibrium prevalence of the infection when nobody is treated. Since $T(t) \to T^*$, system (1) is asymptotically autonomous, and its limit system in the variables $(I, H)$ is

$$\frac{dI}{dt} = \beta I(1 - I) - \gamma I - \frac{\kappa H I}{1 + bI}, \qquad \frac{dH}{dt} = \pi - (m + \varepsilon I)H, \tag{3}$$

on $\Gamma = \{(I, H): 0 \le I \le 1,\ H \ge 0\}$.

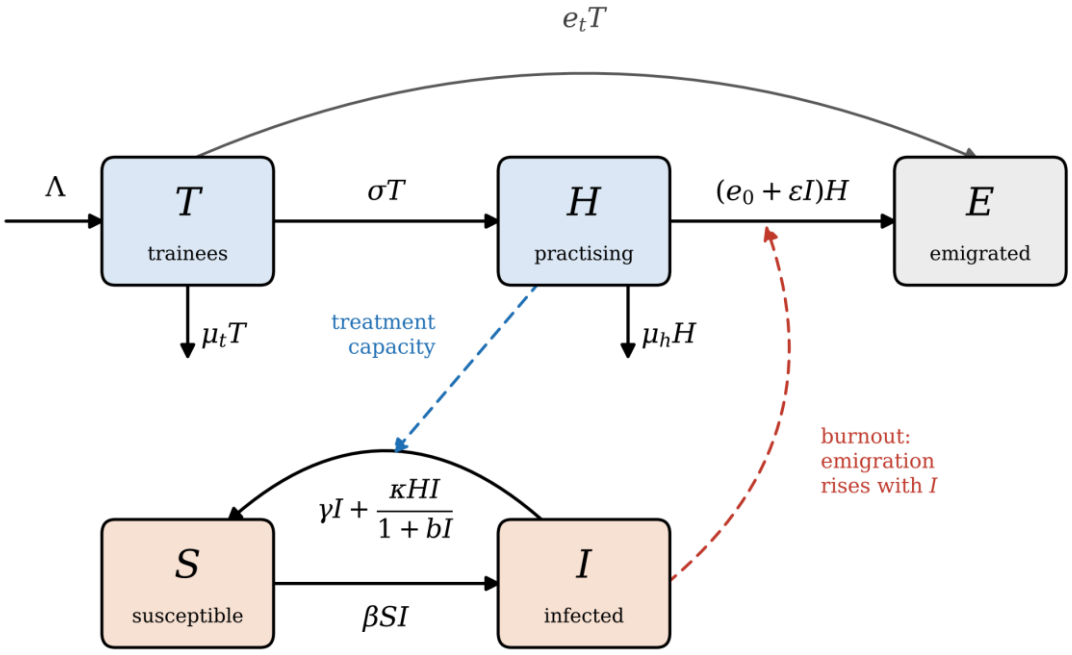



**Figure 1.** Flow diagram of model (1). Solid arrows are flows between compartments. The dashed blue arrow shows that the practising workforce sets the treatment rate, and the dashed red arrow shows that prevalence raises the emigration rate of practising workers.

### 2.2 Parameter values and numerical methods

Table 1 lists the baseline parameter values. Time is measured in years. The values are assumptions chosen so that the disease is controlled at baseline ($\mathcal{R}_0 = 0.75$) with a disease-free workforce of 20 per 10,000; they illustrate the theorems and are not estimates for a particular country or infection.

**Table 1.** Baseline parameter values (all values are assumptions made for illustration).

| Symbol | Description | Value | Unit |
|---|---|---|---|
| $\beta$ | Transmission rate | 3.0 | per year |
| $\gamma$ | Clearance rate without treatment | 1.0 | per year |
| $\kappa$ | Treatment rate per unit density of health workers | 0.15 | per (worker per 10,000) per year |
| $b$ | Saturation constant of treatment | 0 (varied from 0 to 1.4) | dimensionless |
| $\Lambda$ | Training intake | 2.0 | workers per 10,000 per year |
| $\sigma$ | Rate of qualification (training lasts 5 years) | 0.2 | per year |

| Symbol | Description | Value | Unit |
|---|---|---|---|
| $\mu_t$ | Rate of leaving training | 0.02 | per year |
| $e_t$ | Emigration rate of trainees | 0.02 | per year |
| $\mu_h$ | Exit rate of practising workers (career of 30 years) | 1/30 | per year |
| $e_0$ | Baseline emigration rate of practising workers | 0.05 | per year |
| $\varepsilon$ | Burnout sensitivity of emigration | 0.4 | per year per unit prevalence |

Every symbolic identity used in the proofs was checked with SymPy, including the reproduction number, the derivatives of the treatment function, the entries, determinant and trace of the Jacobian, the Dulac divergence, the centre manifold coefficients and the closed-form thresholds of Theorem 7. Simulations of (1) used the LSODA integrator in SciPy with relative tolerance $10^{-9}$. Equilibria were computed by locating sign changes of the function $h$ defined in (17) on a grid of 4,000 points and refining them with Brent's method. To check the closed-form thresholds independently, I computed $e_0^c$ and $\Lambda_c$ as roots of $\mathcal{R}_0 - 1$, and the folds $e_0^{sn}$ and $\Lambda_{sn}$ as roots of $\max_I h$, using bounded scalar optimization and Brent's method with tolerance $10^{-14}$. For the hysteresis experiment I increased and then decreased $e_0$ in 81 steps between 0.04 and 0.12, integrating for 400 years at each step from the end state of the previous step. To represent imported cases, the prevalence was reset to $10^{-3}$ at the start of a step whenever it had fallen below that value. For the global sensitivity analysis I drew 1,000 Latin hypercube samples, varied each parameter uniformly within 50% of its baseline value (with $0 \le b \le 1.5$ and $0 \le \varepsilon \le 0.8$), and computed partial rank correlation coefficients (PRCC) as described by Marino et al. [11].

## 3 Results and discussion

### 3.1 Basic properties

**Lemma 1.** *The set $\Omega = \{(T, I, H, E): T \ge 0,\ 0 \le I \le 1,\ H \ge 0,\ E \ge 0\}$ is positively invariant for (1), and every solution starting in $\Omega$ exists for all $t \ge 0$. Moreover $T(t) = T^* + (T(0) - T^*)e^{-k_t t}$,*

$$\limsup_{t\to\infty} I(t) \le I_{\max}, \qquad \frac{\pi}{m + \varepsilon I_{\max}} \le \liminf_{t\to\infty} H(t) \le \limsup_{t\to\infty} H(t) \le H_0. \tag{4}$$

*Proof.* The right-hand side of (1) is locally Lipschitz, so solutions exist and are unique on a maximal interval. The $T$-equation is linear and gives the stated formula. The face $I = 0$ is invariant, and on $I = 1$ I have $dI/dt = -\gamma - \kappa H/(1 + b) < 0$, so $I$ cannot leave $[0,1]$. Since $dH/dt \ge -(\mu_h + e_0 + \varepsilon)H$ whenever $T \ge 0$, $H$ stays non-negative, and $E$ is non-decreasing. For the bound on $I$, I drop the non-positive treatment term. If $\beta > \gamma$,

$$\frac{dI}{dt} \le \beta I(1 - I) - \gamma I = \beta I(I_{\max} - I), \tag{5}$$

so comparison with the logistic equation $\dot{u} = \beta u(I_{\max} - u)$ gives $\limsup I \le I_{\max}$; if $\beta \le \gamma$, then $dI/dt \le -\beta I^2$ and $I(t) \to 0 = I_{\max}$. For the workforce, the inequalities

$$\sigma T(t) - \big(m + \varepsilon(I_{\max} + \delta)\big)H \le \frac{dH}{dt} \le \sigma T(t) - mH, \tag{6}$$

where the left inequality holds for $t$ large enough and any fixed $\delta > 0$, compare $H$ with solutions of linear equations whose forcing $\sigma T(t)$ tends to $\pi$. This gives $\limsup H \le \pi/m = H_0$, so solutions are bounded and exist for all time, and $\liminf H \ge \pi/\big(m + \varepsilon(I_{\max} + \delta)\big)$. Letting $\delta \to 0$ completes the proof. ■

### 3.2 Reproduction number and critical workforce

Setting $I = 0$ in (1) and putting the derivatives of $T$ and $H$ to zero gives $\Lambda - k_t T = 0$ and $\sigma T - mH = 0$, so system (1) has the disease-free equilibrium

$$P_0 = (T^*, 0, H_0), \qquad T^* = \frac{\Lambda}{k_t}, \qquad H_0 = \frac{\sigma T^*}{m} = \frac{\sigma \Lambda}{k_t m}. \tag{7}$$

**Theorem 1.** *The basic reproduction number of (1) is*

$$\mathcal{R}_0 = \frac{\beta}{\gamma + \kappa H_0} = \frac{\beta\, m\, k_t}{\gamma\, m\, k_t + \kappa\sigma\Lambda}. \tag{8}$$

*The equilibrium $P_0$ is locally asymptotically stable if $\mathcal{R}_0 < 1$ and unstable if $\mathcal{R}_0 > 1$.*

*Proof.* The only infected compartment is $I$. Following van den Driessche and Watmough [18], I split its equation into the rate of new infections and the rate of transfer out of $I$,

$$\mathcal{F} = \beta I(1 - I), \qquad \mathcal{V} = \gamma I + \frac{\kappa H I}{1 + bI}, \qquad F = \left.\frac{\partial \mathcal{F}}{\partial I}\right|_{P_0} = \beta, \qquad V = \left.\frac{\partial \mathcal{V}}{\partial I}\right|_{P_0} = \gamma + \kappa H_0. \tag{9}$$

Hence $\mathcal{R}_0 = FV^{-1} = \beta/(\gamma + \kappa H_0)$, and substituting $H_0$ from (7) gives the second form in (8). The Jacobian of (1) in the variables $(T, I, H)$ at $P_0$ is

$$J(P_0) = \begin{pmatrix} -k_t & 0 & 0 \\ 0 & \beta - \gamma - \kappa H_0 & 0 \\ \sigma & -\varepsilon H_0 & -m \end{pmatrix}. \tag{10}$$

It is lower triangular, so its eigenvalues are $-k_t < 0$, $-m < 0$ and $\beta - \gamma - \kappa H_0 = (\gamma + \kappa H_0)(\mathcal{R}_0 - 1)$, which is negative if $\mathcal{R}_0 < 1$ and positive if $\mathcal{R}_0 > 1$. ■

Formula (8) shows that the workforce acts on the threshold only through its disease-free level $H_0 = \sigma\Lambda/(k_t m)$. Solving $\mathcal{R}_0 = 1$ for each policy parameter gives the critical values below.

**Corollary 1.** *Suppose $\beta > \gamma$. Then $\mathcal{R}_0 < 1$ if and only if any one of the following equivalent conditions holds:*

$$H_0 > H_c := \frac{\beta - \gamma}{\kappa}, \qquad e_0 < e_0^c := \frac{\kappa\pi}{\beta - \gamma} - \mu_h, \qquad \Lambda > \Lambda_c := \frac{(\beta - \gamma)\, m\, k_t}{\kappa\sigma}. \tag{11}$$

*If $\beta \le \gamma$, then $\mathcal{R}_0 < 1$ for all parameter values.*

*Proof.* By (8), $\mathcal{R}_0 < 1$ is equivalent to $\beta < \gamma + \kappa H_0$, that is, $H_0 > (\beta - \gamma)/\kappa$. Writing $H_0 = \pi/m$ and $m = \mu_h + e_0$, this becomes

$$\begin{aligned} &\frac{\pi}{\mu_h + e_0} > \frac{\beta - \gamma}{\kappa} \Leftrightarrow \mu_h + e_0 < \frac{\kappa\pi}{\beta - \gamma} \Leftrightarrow e_0 < \frac{\kappa\pi}{\beta - \gamma} - \mu_h, \\ &\frac{\sigma\Lambda}{k_t m} > \frac{\beta - \gamma}{\kappa} \Leftrightarrow \Lambda > \frac{(\beta - \gamma)\, m\, k_t}{\kappa\sigma}. \end{aligned} \tag{12}$$

If $\beta \le \gamma$, then $\beta < \gamma + \kappa H_0$ because $H_0 > 0$. ■

The quantity $H_c$ is the critical workforce: the infection can invade if and only if the disease-free workforce is below $H_c$. The critical emigration rate $e_0^c$ grows linearly with the inflow $\pi$ of new workers, so a larger training programme allows the system to tolerate more emigration. To compare policy levers I use the normalized sensitivity index $\Upsilon_p^{\mathcal{R}_0} = (\partial\mathcal{R}_0/\partial p)(p/\mathcal{R}_0)$ [9]. Writing $\mathcal{R}_0 = \beta/(\gamma + \kappa\pi/m)$ and differentiating,

$$\begin{aligned} &\frac{\partial\mathcal{R}_0}{\partial\Lambda} = -\frac{\beta\kappa\pi/(m\Lambda)}{(\gamma + \kappa\pi/m)^2}, \qquad \frac{\partial\mathcal{R}_0}{\partial e_0} = \frac{\partial\mathcal{R}_0}{\partial\mu_h} = \frac{\beta\kappa\pi/m^2}{(\gamma + \kappa\pi/m)^2}, \\ &\Upsilon_\Lambda^{\mathcal{R}_0} = -\frac{\kappa H_0}{\gamma + \kappa H_0}, \qquad \Upsilon_{e_0}^{\mathcal{R}_0} = \frac{e_0}{m}\,\frac{\kappa H_0}{\gamma + \kappa H_0}, \qquad \Upsilon_{\mu_h}^{\mathcal{R}_0} = \frac{\mu_h}{m}\,\frac{\kappa H_0}{\gamma + \kappa H_0}. \end{aligned} \tag{13}$$

where I used $\partial\pi/\partial\Lambda = \pi/\Lambda$ and $\partial m/\partial e_0 = \partial m/\partial\mu_h = 1$. At the baseline values, $\kappa H_0/(\gamma + \kappa H_0) = 3/4$ and $e_0/m = 0.6$, so a 10% increase in the training intake lowers $\mathcal{R}_0$ by about 7.5%, whereas a 10% decrease in the baseline emigration rate lowers it by about 4.5%.

The threshold $\mathcal{R}_0 < 1$ guarantees only local stability, because the workforce shrinks when prevalence rises. The next result gives a computable condition for global extinction.

**Theorem 2.** *Define*

$$\mathcal{R}_0^{⍰} = \frac{\beta}{\gamma + \frac{\kappa\pi}{(m+\varepsilon I_{\max})(1+bI_{\max})}}. \tag{14}$$

*Then* $\mathcal{R}_0 \le \mathcal{R}_0^{⍰}$, *with equality if and only if* $\varepsilon I_{\max} = bI_{\max} = 0$. *If* $\mathcal{R}_0^{⍰} < 1$, *then every solution of (1) in* $\Omega$ *satisfies* $I(t) \to 0$, $T(t) \to T^*$ *and* $H(t) \to H_0$.

*Proof.* The denominator of (14) is at most $\gamma + \kappa\pi/m$, the denominator of (8), with equality exactly when $\varepsilon I_{\max} = bI_{\max} = 0$. If $\beta \le \gamma$, then $I(t) \to 0$ by Lemma 1. Let $\beta > \gamma$ and $\mathcal{R}_0^{⍰} < 1$, that is, $\beta - \gamma - \kappa\pi/\big((m + \varepsilon I_{\max})(1 + bI_{\max})\big) < 0$. By continuity there is $\delta > 0$ such that

$$\eta := \beta - \gamma - \frac{\kappa}{1 + b(I_{\max} + \delta)}\left(\frac{\pi}{m + \varepsilon(I_{\max} + \delta)} - \delta\right) < 0. \tag{15}$$

By Lemma 1 there is $t_0$ such that $I(t) \le I_{\max} + \delta$ and $H(t) \ge \pi/\big(m + \varepsilon(I_{\max} + \delta)\big) - \delta$ for $t \ge t_0$. Since $\beta(1 - I) \le \beta$ and $1 + bI \le 1 + b(I_{\max} + \delta)$, the $I$-equation gives $dI/dt \le \eta I$ for $t \ge t_0$, so $I(t) \le I(t_0)e^{\eta(t-t_0)} \to 0$. The $H$-equation is then asymptotic to $dH/dt = \pi - mH$, and $H(t) \to H_0$. ■

### 3.3 Endemic equilibria and burnout-driven backward bifurcation

An endemic equilibrium of (1) has $T = T^*$ and $0 < I^* \le 1$. Setting $dH/dt = 0$ and $dI/dt = 0$ and dividing the second equation by $I^*$ gives

$$\begin{aligned} H^* &= \frac{\pi}{m + \varepsilon I^*}, \\ \beta(1 - I^*) - \gamma - \frac{\kappa H^*}{1 + bI^*} &= 0. \end{aligned} \tag{16}$$

Substituting the first relation into the second shows that $I^*$ is a zero of

$$h(I) = L(I) - G(I), \qquad L(I) = \beta(1 - I) - \gamma, \qquad G(I) = \frac{\kappa\pi}{(m + \varepsilon I)(1 + bI)}. \tag{17}$$

The function $G$ is the per-capita treatment rate at equilibrium when the prevalence is $I$, and $L$ is the net per-capita growth rate of the infection without treatment. Endemic equilibria are therefore the intersections of the straight line $L$ with the curve $G$.

**Lemma 2.** *If* $\varepsilon + b > 0$, *then* $G$ *is strictly decreasing and strictly convex on* $[0,1]$, *so* $h$ *is strictly concave; if* $\varepsilon = b = 0$, *then* $h$ *is linear with slope* $-\beta$. *Moreover*

$$h(0) = (\gamma + \kappa H_0)(\mathcal{R}_0 - 1), \qquad h'(0) = \kappa H_0\left(b + \frac{\varepsilon}{m}\right) - \beta, \qquad h(I) < 0 \text{ for } I \ge I_{\max}. \tag{18}$$

*Proof.* Differentiating $G$ twice gives

$$\begin{aligned} G'(I) &= -\frac{\kappa\pi[\varepsilon(1 + bI) + b(m + \varepsilon I)]}{(m + \varepsilon I)^2(1 + bI)^2} = -G(I)\left(\frac{\varepsilon}{m + \varepsilon I} + \frac{b}{1 + bI}\right), \\ G''(I) &= \frac{2\kappa\pi[\varepsilon^2(1 + bI)^2 + \varepsilon b(m + \varepsilon I)(1 + bI) + b^2(m + \varepsilon I)^2]}{(m + \varepsilon I)^3(1 + bI)^3}. \end{aligned} \tag{19}$$

Every term in the bracket of $G''$ is non-negative and the bracket is positive when $\varepsilon + b > 0$, so $G'' > 0$ and $G' < 0$ on $[0,1]$. Since $L'' = 0$, I get $h'' = -G'' < 0$. If $\varepsilon = b = 0$, then $G$ is constant and $h' = -\beta$. At $I = 0$ I have $G(0) = \kappa\pi/m = \kappa H_0$, so $h(0) = \beta - \gamma - \kappa H_0 = (\gamma + \kappa H_0)(\mathcal{R}_0 - 1)$, and $h'(0) = -\beta - G'(0) = -\beta + \kappa H_0(\varepsilon/m + b)$. For $I \ge I_{\max}$ I have $L(I) \le 0 < G(I)$. ■

**Theorem 3.** *The number of endemic equilibria of (1) is as follows. (a) If* $\mathcal{R}_0 > 1$, *there is exactly one, and it satisfies* $h'(I^*) < 0$. *(b) If* $\mathcal{R}_0 = 1$, *there is one if* $h'(0) > 0$ *and none otherwise. (c) If* $\mathcal{R}_0 < 1$, *there are none, one or two; two endemic equilibria* $I_1 < I_2$ *satisfy* $h'(I_1) > 0 > h'(I_2)$ *and can exist only if* $h'(0) > 0$.

*Proof.* By Lemma 2 all zeros of $h$ lie in the open interval $(0, I_{\max})$, and a strictly concave function has at most two zeros. (a) Here $h(0) > 0 > h(I_{\max})$, so $h$ has a zero. A second zero would force $h$ to be negative between two points where it is non-negative, which is impossible for a concave function with $h(0) > 0$. Concavity gives $h'(I^*) \le \big(h(I^*) - h(0)\big)/I^* = -h(0)/I^* < 0$. (b) Here $h(0) = 0$. If $h'(0) > 0$, then $h$ is positive near 0 and negative at $I_{\max}$, so it has exactly one zero; if $h'(0) \le 0$, then $h < 0$ for $0 < I \le I_{\max}$ by

strict concavity (or linearity). (c) Here $h(0) < 0$. If $h$ has two zeros $I_1 < I_2$, then $h > 0$ between them and strict concavity gives $h'(I_1) > 0 > h'(I_2)$; since $h'$ is decreasing, $h'(0) > h'(I_1) > 0$. ■

I now take the baseline emigration rate $e_0$ as the bifurcation parameter and write $h(I; e_0)$. By Corollary 1, $\mathcal{R}_0 = 1$ exactly at $e_0 = e_0^c$, where $m = m_c := \kappa\pi/(\beta - \gamma)$ and $\kappa H_0 = \kappa\pi/m_c = \beta - \gamma$. Substituting these values into (18) gives

$$\begin{aligned} h'(0; e_0^c) &= (\beta - \gamma)\left(b + \frac{\varepsilon}{m_c}\right) - \beta = \beta(\Psi_c - 1), \qquad \Psi_c := I_{\max}\left(b + \frac{\varepsilon}{m_c}\right) \\ &= bI_{\max} + \frac{\varepsilon I_{\max}}{m_c}, \end{aligned} \tag{20}$$

where I used $(\beta - \gamma)/\beta = I_{\max}$. The index $\Psi_c$ decides the direction of the bifurcation.

**Theorem 4.** *Suppose $\beta > \gamma$. (a) If $\Psi_c \le 1$, system (1) has no endemic equilibrium for $0 \le e_0 \le e_0^c$ and exactly one for $e_0 > e_0^c$; the bifurcation at $e_0^c$ is forward. (b) If $\Psi_c > 1$, the bifurcation at $e_0^c$ is backward, and there is a unique $e_0^{sn}$ with $0 \le e_0^{sn} < e_0^c$ and the following property: for $e_0^{sn} < e_0 < e_0^c$ there are two endemic equilibria; for $e_0 > e_0^c$ there is exactly one; and, if $e_0^{sn} > 0$, there is no endemic equilibrium for $0 \le e_0 < e_0^{sn}$ and one double equilibrium at $e_0 = e_0^{sn}$.*

*Proof.* Since $m = \mu_h + e_0$ and $\partial G/\partial m = -G/(m + \varepsilon I) < 0$, the function $h(I; e_0)$ is strictly increasing in $e_0$ for every $0 < I \le 1$. At $e_0 = e_0^c$ I have $h(0) = 0$ and, by (20), $h'(0) = \beta(\Psi_c - 1)$. (a) If $\Psi_c \le 1$, then $h'(0; e_0^c) \le 0$, so $h(I; e_0^c) < 0$ for $0 < I \le I_{\max}$ by Lemma 2, and monotonicity gives $h(I; e_0) < h(I; e_0^c) < 0$ for all $e_0 < e_0^c$. The case $e_0 > e_0^c$ is Theorem 3(a). (b) Let $M(e_0) = \max\{h(I; e_0): 0 \le I \le I_{\max}\}$. Then $M$ is continuous, and it is strictly increasing: if $M(e_0) = h(\hat{I}; e_0)$ and $e_0 < \tilde{e}_0$, then $M(e_0) < h(\hat{I}; \tilde{e}_0) \le M(\tilde{e}_0)$. Since $h'(0; e_0^c) > 0$, I have $M(e_0^c) > 0$. Let $e_0^{sn}$ be the zero of $M$ below $e_0^c$ if $M(0) < 0$, and $e_0^{sn} = 0$ otherwise. For $e_0^{sn} < e_0 < e_0^c$ I have $h(0; e_0) < 0 < M(e_0)$ and $h(I_{\max}; e_0) < 0$, so $h$ has exactly two zeros by strict concavity. If $M(e_0) < 0$ there is no zero, and if $M(e_0) = 0$ the maximum point is a double zero. ■

The index $\Psi_c$ has a direct interpretation. The term $bI_{\max}$ measures how much treatment saturates at the untreated peak prevalence. The term $\varepsilon I_{\max}/m_c$ is the ratio of the extra emigration rate caused by burnout at the untreated peak prevalence to the exit rate of health workers at the threshold. If $b = 0$, the bifurcation is backward exactly when $\varepsilon I_{\max} > m_c$, that is, when an uncontrolled epidemic would more than double the rate at which health workers leave. Burnout-driven emigration is therefore enough to produce a backward bifurcation, with no saturation of treatment. If $\varepsilon = 0$, the condition reduces to $bI_{\max} > 1$, which concerns treatment saturation alone.

**Remark 1.** The direction of the bifurcation can be confirmed with the centre manifold method of Castillo-Chavez and Song [5]. Take $\beta$ as the bifurcation parameter; $\mathcal{R}_0 = 1$ at $\beta^* = \gamma + \kappa H_0$. Write $x = (T, I, H)$ and let $f_1, f_2, f_3$ be the right-hand sides of (1). At $\beta = \beta^*$ the matrix (10) has a simple zero eigenvalue with right and left eigenvectors

$$w = \left(0,\ 1,\ -\frac{\varepsilon H_0}{m}\right)^T, \qquad v = (0,\ 1,\ 0), \qquad v\,w = 1. \tag{21}$$

At $P_0$ the only non-zero second derivatives of $f_2$ are $\partial^2 f_2/\partial I^2 = -2\beta + 2b\kappa H_0$, $\partial^2 f_2/\partial I\,\partial H = -\kappa$ and $\partial^2 f_2/\partial I\,\partial\beta = 1$. The bifurcation coefficients are therefore

$$\begin{aligned} a &= \sum_{k,i,j} v_k\, w_i w_j \frac{\partial^2 f_k}{\partial x_i\,\partial x_j}(P_0) = w_2^2(-2\beta^* + 2b\kappa H_0) + 2w_2 w_3(-\kappa), \\ a &= 2\left[\kappa H_0\left(b + \frac{\varepsilon}{m}\right) - \beta^*\right], \\ c &= \sum_{k,i} v_k\, w_i \frac{\partial^2 f_k}{\partial x_i\,\partial\beta}(P_0) = w_2 = 1 > 0. \end{aligned} \tag{22}$$

At $\beta = \beta^*$ I have $\kappa H_0 = \beta^* - \gamma$, so $a = 2\beta^*(\Psi - 1)$ with $\Psi = (1 - \gamma/\beta^*)(b + \varepsilon/m)$, the index (20) evaluated at this threshold. Since $c > 0$, Theorem 4.1 of Castillo-Chavez and Song [5] shows that the bifurcation is backward when $a > 0$ and forward when $a < 0$, in agreement with Theorem 4.

### 3.4 Stability and global dynamics

**Theorem 5.** *Let $(T^*, I^*, H^*)$ be an endemic equilibrium of (1). The eigenvalues of the Jacobian are $-k_t$ and the eigenvalues of the Jacobian $J^*$ of (3) at $(I^*, H^*)$, which satisfies*

$$\det J^* = -I^*(m+\varepsilon I^*)\,h'(I^*), \qquad \mathrm{tr}J^* = \frac{I^*(b(\beta-\gamma)-\beta-2b\beta I^*)}{1+bI^*} - (m+\varepsilon I^*). \tag{23}$$

*Hence the equilibrium is a saddle if $h'(I^*) > 0$. If $h'(I^*) < 0$ and $b(\beta-\gamma) \le \beta$, it is locally asymptotically stable.*

*Proof.* The $T$-equation does not depend on $(I, H)$, so the Jacobian of (1) is block triangular with the block $-k_t$ and the block

$$J^* = \begin{pmatrix} \beta(1-2I^*) - \gamma - \dfrac{\kappa H^*}{(1+bI^*)^2} & -\dfrac{\kappa I^*}{1+bI^*} \\ -\varepsilon H^* & -(m+\varepsilon I^*) \end{pmatrix}. \tag{24}$$

Write $G^* = G(I^*) = \kappa H^*/(1+bI^*)$. The equilibrium relation (16) reads $\beta(1-I^*) - \gamma = G^*$. Using it to eliminate $\gamma$ from the first entry,

$$\begin{aligned} J_{11} &= -\beta I^* + G^* - \frac{G^*}{1+bI^*} = -\beta I^* + \frac{bI^*G^*}{1+bI^*}, \\ J_{11} &= I^*\,\frac{-\beta(1+bI^*) + b(\beta(1-I^*)-\gamma)}{1+bI^*}, \\ J_{11} &= \frac{I^*(b(\beta-\gamma)-\beta-2b\beta I^*)}{1+bI^*}. \end{aligned} \tag{25}$$

Adding $J_{22} = -(m+\varepsilon I^*)$ gives the trace in (23). For the determinant, $J_{12}J_{21} = \varepsilon I^* G^*$, so

$$\det J^* = J_{11}J_{22} - J_{12}J_{21} = \beta I^*(m+\varepsilon I^*) - \frac{bI^*G^*(m+\varepsilon I^*)}{1+bI^*} - \varepsilon I^* G^*. \tag{26}$$

On the other hand, by (19), $h'(I^*) = -\beta - G'(I^*) = -\beta + G^*\big(\varepsilon/(m+\varepsilon I^*) + b/(1+bI^*)\big)$. Multiplying by $-I^*(m+\varepsilon I^*)$ reproduces the right-hand side of (26), which proves the formula for $\det J^*$. If $h'(I^*) > 0$, then $\det J^* < 0$ and the equilibrium is a saddle. If $h'(I^*) < 0$, then $\det J^* > 0$; if also $b(\beta-\gamma) \le \beta$, then $b(\beta-\gamma) - \beta - 2b\beta I^* < 0$, so $\mathrm{tr}J^* < 0$ and both eigenvalues have negative real parts. ■

By Theorems 3 and 5, the unique endemic equilibrium for $\mathcal{R}_0 > 1$ and the upper equilibrium $I_2$ in the backward case are stable when $b(\beta-\gamma) \le \beta$, and the lower equilibrium $I_1$ is always a saddle. Under the same condition, periodic solutions are excluded.

**Theorem 6.** *Suppose $\beta > \gamma$, $b(\beta-\gamma) \le \beta$ and $e_0 \notin \{e_0^{sn}, e_0^c\}$. Then $\big(T(t), I(t), H(t)\big)$ converges to an equilibrium for every solution of (1) in $\Omega$. More precisely: (a) if $e_0 > e_0^c$ and $I(0) > 0$, the solution converges to the endemic equilibrium; (b) if $e_0 < e_0^c$ and there is no endemic equilibrium (in particular if $\Psi_c \le 1$, or if $\Psi_c > 1$ and $e_0 < e_0^{sn}$), the solution converges to $P_0$; (c) if $\Psi_c > 1$ and $e_0^{sn} < e_0 < e_0^c$, then $P_0$ and the upper endemic equilibrium are both locally asymptotically stable, and the solutions that converge to the lower endemic equilibrium form a set with empty interior in $\Omega$.*

*Proof.* Let $f = (f_1, f_2)$ be the right-hand side of (3) and take the Dulac function $\phi(I,H) = (1+bI)/(IH)$ on the interior of $\Gamma$. Then

$$\begin{aligned} \phi f_1 &= \frac{(1+bI)(\beta(1-I)-\gamma)}{H} - \kappa, \qquad \phi f_2 = (1+bI)\left(\frac{\pi}{IH} - \frac{m+\varepsilon I}{I}\right), \\ \frac{\partial(\phi f_1)}{\partial I} &= \frac{b(\beta(1-I)-\gamma) - \beta(1+bI)}{H} = \frac{b(\beta-\gamma)-\beta-2b\beta I}{H}, \qquad \frac{\partial(\phi f_2)}{\partial H} \\ &= -\frac{(1+bI)\pi}{IH^2}, \end{aligned} \tag{27}$$

so that

$$\frac{\partial(\phi f_1)}{\partial I} + \frac{\partial(\phi f_2)}{\partial H} = \frac{b(\beta-\gamma)-\beta-2b\beta I}{H} - \frac{(1+bI)\pi}{IH^2} < 0 \quad \text{when} \quad b(\beta-\gamma) \le \beta. \tag{28}$$

By Dulac's criterion [15], system (3) has no periodic orbit, homoclinic loop or heteroclinic cycle in the interior of $\Gamma$. The face $I = 0$ is invariant, every solution on it converges to $(0, H_0)$, and $(0, H_0)$ is the only equilibrium on it, so a cyclic chain of equilibria would have to bound a region in the interior of $\Gamma$, which (28) excludes. Since the rectangle $[0,1] \times [0, H_0 + 1]$ is absorbing, the Poincaré-Bendixson theorem shows that every solution of (3) converges to one of its finitely many equilibria, all of which are hyperbolic because $e_0 \notin \{e_0^{sn}, e_0^c\}$ (Theorems 1, 3 and 5). Now consider (1). The pair $(I, H)$ solves an asymptotically autonomous planar system whose limit system is (3), because $\sigma T(t) \to \pi$ exponentially. The $\omega$-limit set of $(I, H)$ is compact, connected, invariant and chain recurrent for (3) [12, 17]. Since every orbit of (3) converges to one of finitely many hyperbolic equilibria and there is no cyclic chain of equilibria, such a set consists of a single equilibrium [26, Chapter 1]. (a) The only equilibria are $P_0$ and the endemic one. If $I(0) > 0$ and $(I, H) \to (0, H_0)$, then $I(t) > 0$ for all $t$ and $(dI/dt)/I \to \beta - \gamma - \kappa H_0 > 0$, so $I$ is eventually increasing, a contradiction. (b) Here $P_0$ is the only equilibrium. (c) Stability of $P_0$ and of the upper equilibrium follows from Theorems 1 and 5. The lower equilibrium is a hyperbolic saddle of the three-dimensional autonomous system $(T, I, H)$ with a one-dimensional unstable manifold, so its stable manifold is two-dimensional and has empty interior. ■

The condition $b(\beta - \gamma) \le \beta$ in Theorems 5 and 6 has a plain meaning. Since $I_{\max} = 1 - \gamma/\beta$, it is equivalent to $bI_{\max} \le 1$, that is, $1/(1 + bI_{\max}) \ge 1/2$: at the prevalence that an untreated epidemic would reach, saturation lowers the treatment rate per infected person to no less than half of its value at a light caseload. At the baseline values $\beta = 3$ and $\gamma = 1$ the condition allows $b \le 1.5$, which covers every value of $b$ used in this paper. It excludes strongly saturating treatment, for which the Dulac argument does not apply and periodic solutions are not ruled out. Under the condition and with $\varepsilon = 0$, the index (20) is $\Psi_c = bI_{\max} \le 1$, so the bifurcation is forward; within the range covered by Theorem 6, a backward bifurcation therefore requires burnout-driven emigration.

### 3.5 Explicit thresholds without saturation

When treatment does not saturate ($b = 0$), the equation $h = 0$ becomes quadratic and the fold can be computed explicitly. Write $D = \beta - \gamma$. Multiplying $h$ by $m + \varepsilon I > 0$ and expanding,

$$\begin{aligned} &(m + \varepsilon I)\, h(I) = (\beta - \beta I - \gamma)(m + \varepsilon I) - \kappa\pi = -\mathcal{A} I^2 + \mathcal{B}_m I + \mathcal{C}_m, \\ &\mathcal{A} = \beta\varepsilon, \qquad \mathcal{B}_m = \varepsilon D - \beta m, \qquad \mathcal{C}_m = mD - \kappa\pi. \end{aligned} \tag{29}$$

The discriminant of this quadratic simplifies to a difference of squares:

$$\begin{aligned} &\mathcal{B}_m^2 + 4\mathcal{A}\mathcal{C}_m = \varepsilon^2 D^2 - 2\beta\varepsilon D m + \beta^2 m^2 + 4\beta\varepsilon m D - 4\beta\varepsilon\kappa\pi, \\ &\mathcal{B}_m^2 + 4\mathcal{A}\mathcal{C}_m = (\varepsilon D + \beta m)^2 - 4\beta\varepsilon\kappa\pi. \end{aligned} \tag{30}$$

**Theorem 7.** *Let $b = 0$ and $\beta > \gamma$. Then*

$$\Psi_c = \frac{\varepsilon D^2}{\beta\kappa\pi}, \qquad e_0^c = \frac{\kappa\pi}{D} - \mu_h. \tag{31}$$

*If $\Psi_c > 1$, then*

$$e_0^{sn} = \max\left\{0,\ \frac{2\sqrt{\beta\varepsilon\kappa\pi} - \varepsilon D}{\beta} - \mu_h\right\}, \qquad I_{sn} = \frac{1}{\beta}\left(D - \sqrt{\frac{\beta\kappa\pi}{\varepsilon}}\right), \tag{32}$$

*where $I_{sn}$ is the prevalence at the fold when $e_0^{sn} > 0$. For $e_0^{sn} < e_0 < e_0^c$ the two endemic prevalences are*

$$I_{1,2} = \frac{\mathcal{B}_m \mp \sqrt{(\varepsilon D + \beta m)^2 - 4\beta\varepsilon\kappa\pi}}{2\beta\varepsilon}. \tag{33}$$

*If $e_0^{sn} > 0$, the width of the hysteresis interval and the prevalence of the stable endemic equilibrium at $e_0 = e_0^c$ are*

$$\Delta := e_0^c - e_0^{sn} = \frac{\left(\sqrt{\beta\kappa\pi} - D\sqrt{\varepsilon}\right)^2}{\beta D}, \qquad I_2(e_0^c) = I_{\max}\left(1 - \frac{1}{\Psi_c}\right). \tag{34}$$

*Proof.* Formula (31) follows from (20) with $b = 0$, $I_{\max} = D/\beta$ and $m_c = \kappa\pi/D$, and (33) is the quadratic formula applied to (29) with (30). The two roots merge when the discriminant (30) vanishes. Since $\varepsilon D + \beta m > 0$, this happens at

$$\varepsilon D + \beta m_{sn} = 2\sqrt{\beta\varepsilon\kappa\pi} \Leftrightarrow m_{sn} = \frac{2\sqrt{\beta\varepsilon\kappa\pi} - \varepsilon D}{\beta}, \tag{35}$$

which gives $e_0^{sn} = m_{sn} - \mu_h$ (or 0 if this is negative). The double root is $I_{sn} = \mathcal{B}_{m_{sn}}/(2\mathcal{A})$, and

$$\mathcal{B}_{m_{sn}} = \varepsilon D - \beta m_{sn} = 2\varepsilon D - 2\sqrt{\beta\varepsilon\kappa\pi} = 2\sqrt{\varepsilon}\left(D\sqrt{\varepsilon} - \sqrt{\beta\kappa\pi}\right), \tag{36}$$

which is positive exactly when $\varepsilon D^2 > \beta\kappa\pi$, that is, when $\Psi_c > 1$. Dividing by $2\mathcal{A} = 2\beta\varepsilon$ gives $I_{sn}$ in (32). For the width of the hysteresis interval,

$$\begin{aligned} \Delta &= m_c - m_{sn} = \frac{\kappa\pi}{D} - \frac{2\sqrt{\beta\varepsilon\kappa\pi} - \varepsilon D}{\beta} = \frac{\beta\kappa\pi - 2D\sqrt{\beta\varepsilon\kappa\pi} + \varepsilon D^2}{\beta D}, \\ \Delta &= \frac{\left(\sqrt{\beta\kappa\pi} - D\sqrt{\varepsilon}\right)^2}{\beta D}. \end{aligned} \tag{37}$$

Finally, at $m = m_c$ I have $\mathcal{C}_{m_c} = 0$, so the roots of (29) are 0 and $I_2 = \mathcal{B}_{m_c}/\mathcal{A} = D/\beta - \kappa\pi/(\varepsilon D) = I_{\max}(1 - 1/\Psi_c)$. ■

Formula (34) shows that the hysteresis disappears as $\varepsilon$ decreases to $\beta\kappa\pi/D^2$, where $\Psi_c = 1$, and that the jump in prevalence when control is lost at $e_0^c$ grows with $\Psi_c$. The same computation applies when the training intake is the bifurcation parameter.

**Corollary 2.** *Let $b = 0$, $\beta > \gamma$, and fix $e_0$. Then $\mathcal{R}_0 < 1$ if and only if $\pi > \pi_c := mD/\kappa$. If $\varepsilon D > \beta m$, the system has two endemic equilibria for $\pi_c < \pi < \pi_{sn}$, where*

$$\pi_{sn} = \frac{(\varepsilon D + \beta m)^2}{4\beta\varepsilon\kappa}, \qquad \Lambda_{sn} = \frac{k_t}{\sigma}\,\pi_{sn}. \tag{38}$$

*If $\varepsilon D \le \beta m$, no endemic equilibrium exists for $\pi \ge \pi_c$.*

*Proof.* Setting the discriminant (30) to zero and solving for $\pi$ gives $\pi_{sn}$. Moreover

$$\pi_{sn} - \pi_c = \frac{(\varepsilon D + \beta m)^2 - 4\beta\varepsilon m D}{4\beta\varepsilon\kappa} = \frac{(\varepsilon D - \beta m)^2}{4\beta\varepsilon\kappa} \ge 0. \tag{39}$$

At $\pi = \pi_c$ the index is $\varepsilon D^2/(\beta\kappa\pi_c) = \varepsilon D/(\beta m)$. Since $G$ is increasing in $\pi$, $h$ is strictly decreasing in $\pi$, and the argument of Theorem 4 with $\pi$ in place of $e_0$ gives the result. ■

### 3.6 Numerical results

At the baseline values of Table 1, formulas (2), (11), (8), (14) and (31) give $H_0 = 20$ and $H_c = 13.33$ per 10,000, $\mathcal{R}_0 = 0.75$, $\mathcal{R}_0^{\text{T}} = 1.75$ and $\Psi_c = 2.13$. Table 2 lists the remaining thresholds. For each one it gives the value from the closed-form formula and the value from an independent numerical computation (root finding on $\mathcal{R}_0 - 1$ or on $\max_I h$). The two agree to at least ten significant digits.

**Table 2.** Thresholds at the baseline parameter values: closed-form formula against independent numerical computation.

| Quantity | Formula | Closed form | Numerical |
|---|---|---|---|
| Critical emigration rate $e_0^c$ (per year) | (31) | 0.091667 | 0.091667 |
| Fold point $e_0^{sn}$ (per year) | (32) | 0.065148 | 0.065148 |
| Prevalence at the fold $I_{sn}$ | (32) | 0.210231 | 0.210231 |
| Prevalence jump at $e_0^c$ | (34) | 0.354167 | 0.354167 |
| Width of hysteresis interval $\Delta$ (per year) | (34) | 0.026518 | 0.026518 |
| Critical training intake $\Lambda_c$ (per 10,000 per year) | (11) | 1.333333 | 1.333333 |
| Training intake at the fold $\Lambda_{sn}$ (per 10,000 per year) | (38) | 1.837500 | 1.837500 |

At baseline the infection is controlled ($\mathcal{R}_0 = 0.75$) and, since $e_0 = 0.05 < e_0^{sn}$, no endemic equilibrium exists; Theorem 6(b) then gives global convergence to $P_0$ even though $\mathcal{R}_0^{\boxed{?}} = 1.75 > 1$, so Theorem 2 alone would not decide the outcome. Because $\Psi_c = 2.13 > 1$, a rise in the baseline emigration rate beyond 0.0651 per year creates a stable endemic state while $P_0$ remains stable, and a rise beyond 0.0917 per year makes $P_0$ unstable.

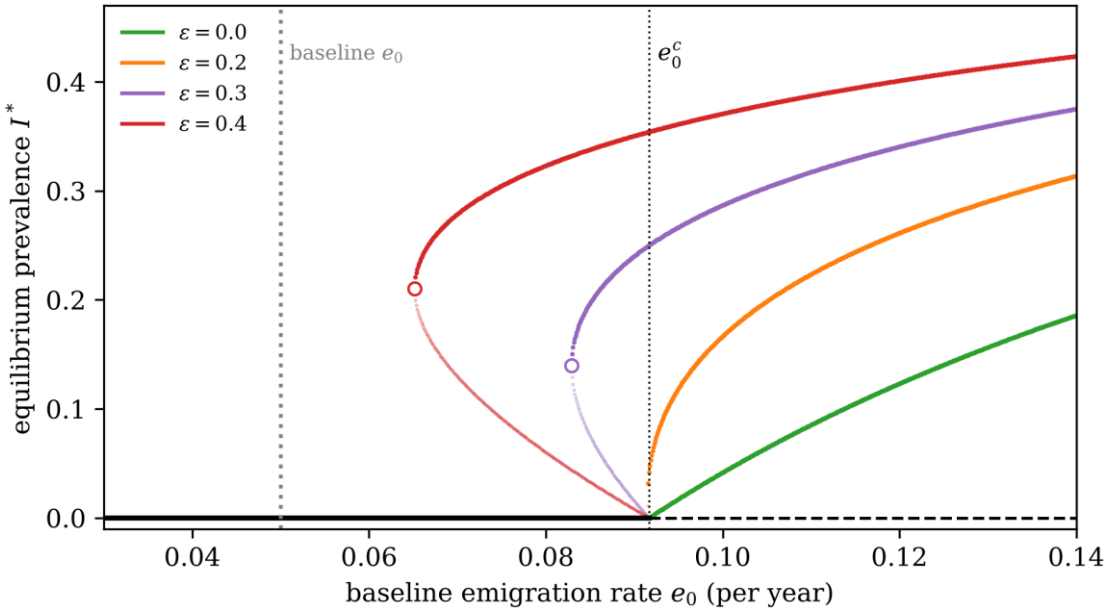



**Figure 2.** Burnout turns a gradual loss of control into an abrupt one: for larger burnout sensitivity a stable endemic state appears before the reproduction number reaches one. Equilibrium prevalence against the baseline emigration rate $e_0$ for four values of the burnout sensitivity $\varepsilon$ ($b = 0$, other values as in Table 1). Heavy dots mark stable equilibria and light dots unstable ones; the black line is the disease-free equilibrium (solid when stable, dashed when unstable). Open circles mark the folds. The bifurcation is forward for $\varepsilon = 0$ and backward for $\varepsilon \geq 0.2$, in agreement with $\Psi_c = 5.33\varepsilon$.

Figure 2 shows the bifurcation diagram in $e_0$. Since $\Psi_c = 5.33\varepsilon$ at the baseline values, the bifurcation is forward for $\varepsilon = 0$ and backward for $\varepsilon = 0.2$, 0.3 and 0.4. The critical value $e_0^c$ does not depend on $\varepsilon$, but the fold moves to the left as $\varepsilon$ grows: for $\varepsilon = 0.4$ the interval of bistability is $(0.0651, 0.0917)$.

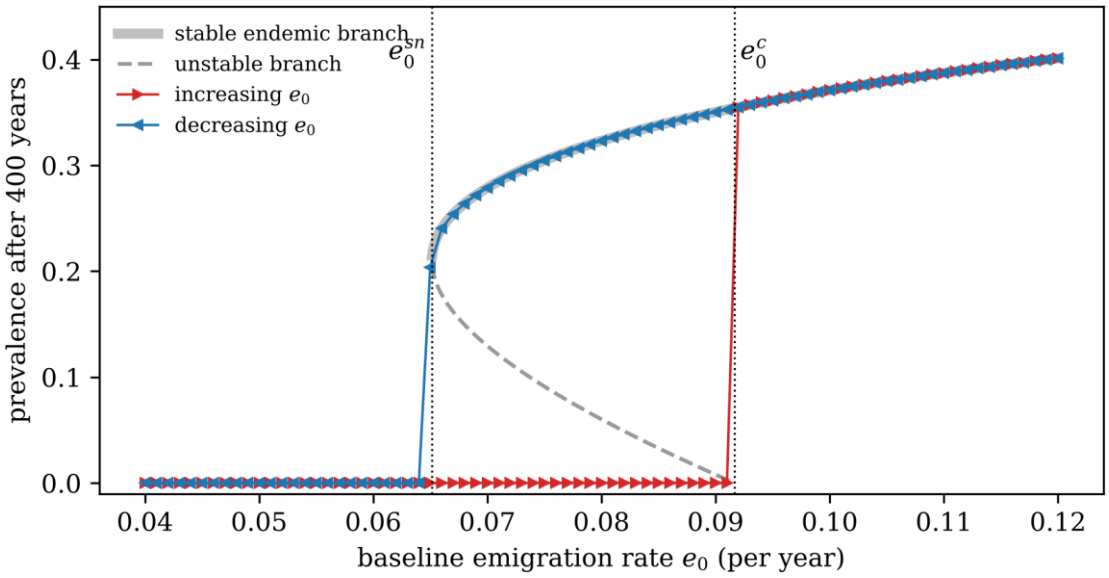



**Figure 3.** Once control is lost, bringing emigration back to the rate at which it was lost does not restore control. Hysteresis obtained by numerical continuation of model (1). The baseline emigration rate is raised from 0.04 to 0.12 (red) and then lowered back (blue); each point is the prevalence after 400 years. The grey curves are the stable (solid) and unstable (dashed) endemic branches from Theorem 7.

Figure 3 shows the hysteresis loop. When $e_0$ is raised, the infection stays near zero until $e_0$ passes $e_0^c = 0.0917$; in the continuation the jump occurs between the steps $e_0 = 0.091$ and $e_0 = 0.092$, and the prevalence reaches about 0.35, as predicted by (34). When $e_0$ is lowered again, the prevalence follows the upper branch and drops to zero between the steps 0.065 and 0.064, which brackets $e_0^{sn} = 0.0651$. Restoring control therefore requires emigration to fall about 29% below the rate at which control was lost.

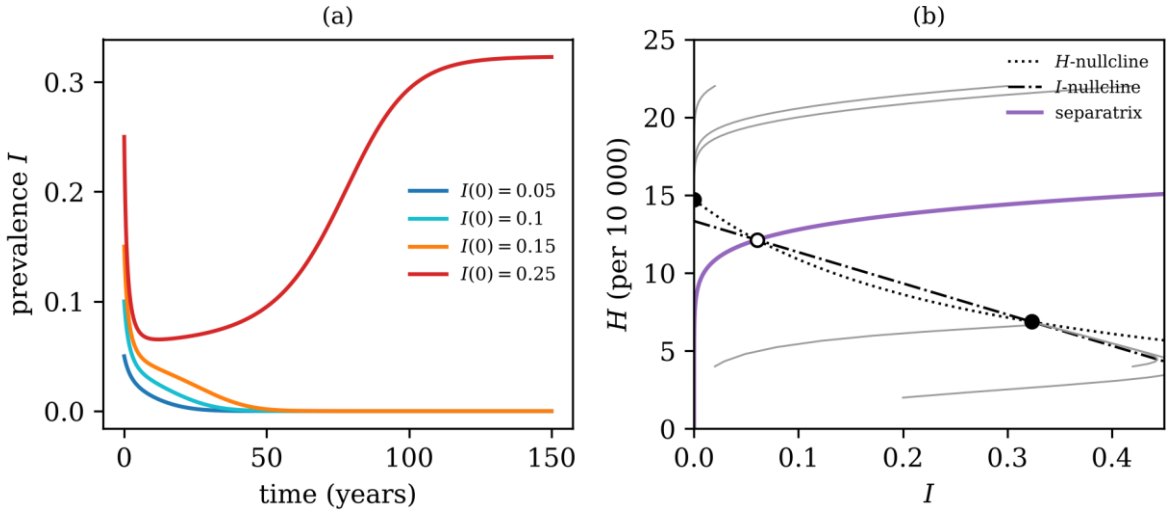



**Figure 4.** Below the threshold, small outbreaks die out but a large outbreak can settle into a lasting endemic state. Bistability at $e_0 = 0.08$ ($\mathcal{R}_0 = 0.936$). (a) Prevalence for four initial prevalences, with $T(0) = T^*$ and $H(0) = 14$. (b) Phase portrait of the limit system (3): the black dots are the stable equilibria $P_0$ and $(0.323, 6.87)$, the open dot is the saddle $(0.060, 12.13)$, and the purple curve is the stable manifold of the saddle, which separates the two basins of attraction.

Figure 4 illustrates Theorem 6(c) at $e_0 = 0.08$, where $\mathcal{R}_0 = 0.936$. Outbreaks that start with prevalence 0.05, 0.10 or 0.15 die out, while an outbreak that starts at 0.25 reduces the workforce enough to settle at the endemic equilibrium with prevalence 0.323 and a workforce of 6.87 per 10,000, about half of the disease-free level of 14.71. Figure 4(a) also shows that the transition can be slow: after an initial decline, prevalence stays below 0.1 for about 50 years before the workforce falls far enough for the infection to take hold.

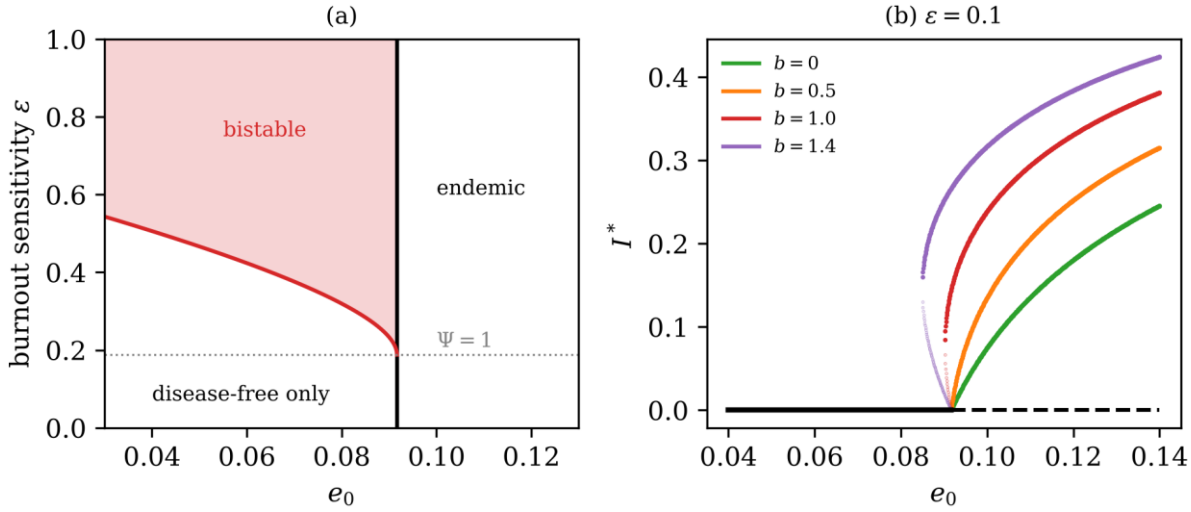



**Figure 5.** Bistability needs a strong enough burnout response (a), and treatment saturation widens it (b). (a) Regions in the $(e_0, \varepsilon)$ plane for $b = 0$: only the disease-free equilibrium (below the red curve and left of $e_0^c$), bistability (shaded), and a stable endemic equilibrium (right of $e_0^c$). The dotted line is $\Psi_c = 1$. (b) Bifurcation diagrams for $\varepsilon = 0.1$ and four values of the saturation constant $b$; all four satisfy $b(\beta - \gamma) \leq \beta$.

Figure 5(a) shows the regions of Theorem 4 in the $(e_0, \varepsilon)$ plane. Bistability requires $\varepsilon > \beta\kappa\pi/D^2 = 0.1875$, and for $\varepsilon$ above about 0.54 it extends to the lower edge $e_0 = 0.03$ of the plotted range. Figure 5(b) shows how saturation interacts with burnout. With $\varepsilon = 0.1$, $\Psi_c = 0.533 + 0.667b$, so the bifurcation is forward for $b = 0$ and $b = 0.5$ and backward for $b = 1.0$ and $b = 1.4$.

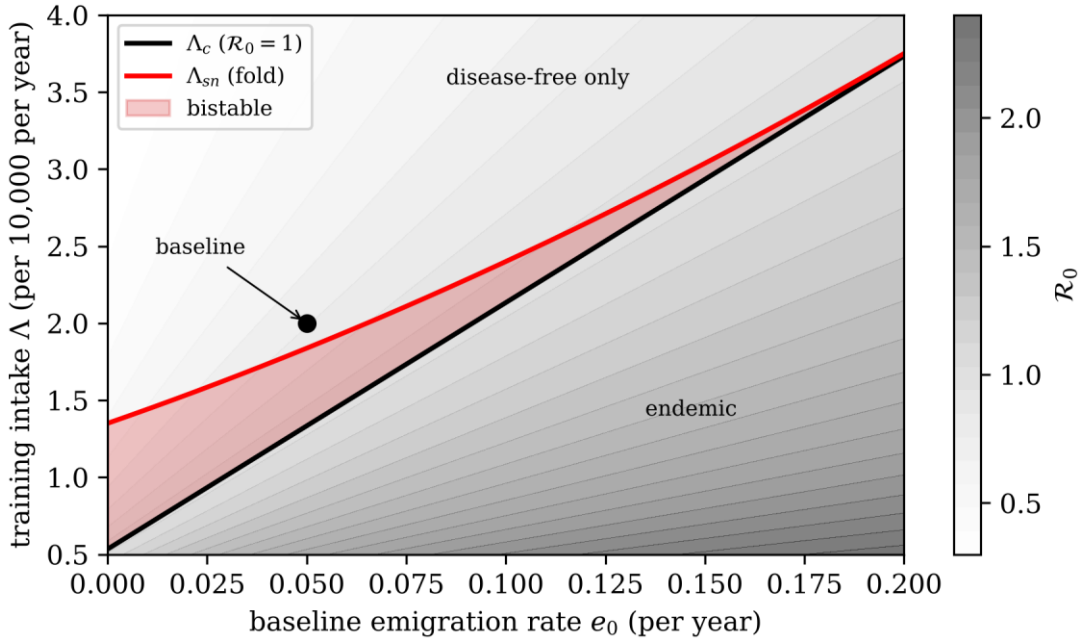



**Figure 6.** Training intake and emigration together decide whether control is secure, at risk of being lost after a large outbreak, or already lost. The policy plane of baseline emigration rate $e_0$ and training intake $\Lambda$ ($b = 0$, other values as in Table 1). Shading shows $\mathcal{R}_0$ from (8). The black line is $\Lambda_c$ from (11) and the red curve is $\Lambda_{sn}$ from (38); between them both the disease-free and the endemic equilibria are stable.

Figure 6 combines the two policy levers. The critical line $\Lambda_c$ rises linearly with $e_0$, since $\Lambda_c = (\beta - \gamma)(\mu_h + e_0)k_t/(\kappa\sigma)$. The fold curve $\Lambda_{sn}$ lies above it and the two meet where $\varepsilon D = \beta m$, that is, at $e_0 = \varepsilon D/\beta - \mu_h = 0.233$. The baseline point lies above both curves, but only by a small margin: at $e_0 = 0.05$ a fall in the training intake from 2.0 to below 1.84 per 10,000 per year would already allow an outbreak to become endemic, although $\mathcal{R}_0$ stays below one until the intake falls below 1.33.

### 3.7 Global sensitivity analysis

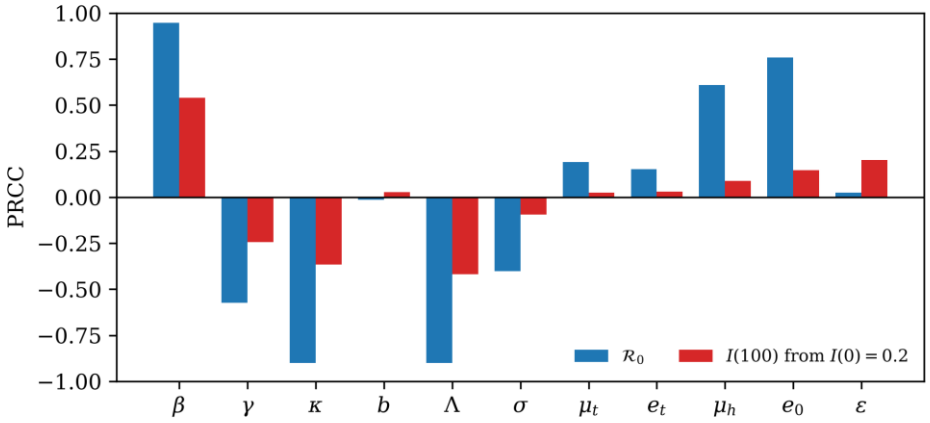



**Figure 7.** Burnout does not change the reproduction number but does change how much infection remains after a large outbreak. Partial rank correlation coefficients of $\mathcal{R}_0$ (blue) and of the prevalence after 100 years starting from $I(0) = 0.2$, $T(0) = T^*$, $H(0) = H_0$ (red), from 1,000 Latin hypercube samples.

Figure 7 shows the PRCC values. For $\mathcal{R}_0$ the most influential parameters are $\beta$ (PRCC 0.95), $\kappa$ $(-0.90)$, $\Lambda$ $(-0.90)$, $e_0$ (0.76) and $\mu_h$ (0.61); the coefficients of $\varepsilon$ and $b$ are close to zero and not significant ($p > 0.4$), as formula (8) predicts. For the prevalence after a large outbreak the picture changes: $\varepsilon$ has a significant positive coefficient (0.20, $p \approx 10^{-10}$), larger than that of $e_0$ (0.15). In 70.6% of the samples $\mathcal{R}_0 < 1$, yet in 7.1% of all samples the infection still persisted after 100 years with prevalence above 0.01 despite $\mathcal{R}_0 < 1$. The reproduction number alone therefore does not predict the outcome of an outbreak when emigration responds to burnout.

### 3.8 Return migration

Assumption (A4) excludes return migration. To see how return changes the results, let emigrated health workers return to practice at rate $\rho \geq 0$ and leave the pool of possible returners, through retirement, death or permanent settlement abroad, at rate $\mu_E > 0$. The equations for $H$ and $E$ in (1) become

$$\frac{dH}{dt} = \sigma T + \rho E - (\mu_h + e_0 + \varepsilon I)H, \qquad \frac{dE}{dt} = e_t T + (e_0 + \varepsilon I)H - (\rho + \mu_E)E, \tag{40}$$

and $E$ now counts the emigrants who may still return; with $\rho = 0$ the equation for $H$ is that of (1). Define

$$\theta = \frac{\mu_E}{\rho + \mu_E}, \quad \tilde{\pi} = \sigma T^* + \frac{\rho\, e_t T^*}{\rho + \mu_E}, \quad \tilde{m} = \mu_h + \theta e_0, \quad \tilde{\varepsilon} = \theta\varepsilon, \quad \widetilde{H}_0 = \frac{\tilde{\pi}}{\tilde{m}}. \tag{41}$$

**Theorem 8.** *Suppose $\rho \geq 0$ and $\mu_E > 0$, and let the other parameters be as in (1). (a) At every equilibrium of system (1) with the equations (40), $T = T^*$ and $H = \tilde{\pi}/(\tilde{m} + \tilde{\varepsilon} I)$. (b) The disease-free equilibrium has $H = \widetilde{H}_0$, its basic reproduction number is $\tilde{\mathcal{R}}_0 = \beta/\big(\gamma + \kappa\widetilde{H}_0\big)$, and it is locally asymptotically stable if $\tilde{\mathcal{R}}_0 < 1$ and unstable if $\tilde{\mathcal{R}}_0 > 1$. (c) The endemic equilibria are the zeros $0 < I \leq 1$ of the function $h$ in (17) with $\pi$, $m$ and $\varepsilon$ replaced by $\tilde{\pi}$, $\tilde{m}$ and $\tilde{\varepsilon}$; hence Lemma 2 and Theorems 3 and 4 hold with these replacements, and the direction of the bifurcation is decided by $\widetilde{\Psi}_c = I_{\max}(b + \tilde{\varepsilon}/\tilde{m}_c)$ with $\tilde{m}_c = \kappa\tilde{\pi}/(\beta - \gamma)$. (d) If $\rho > 0$, then $\widetilde{H}_0 > H_0$ and $\tilde{\mathcal{R}}_0 < \mathcal{R}_0$; if in addition $\varepsilon > 0$, then $\widetilde{\Psi}_c < \Psi_c$.*

*Proof.* (a) The equation for $T$ is unchanged, so $T = T^*$. Setting $dE/dt = 0$ gives $E = (e_t T^* + (e_0 + \varepsilon I)H)/(\rho + \mu_E)$. Substituting this into $dH/dt = 0$ gives $\sigma T^* + \rho e_t T^*/(\rho + \mu_E) - \big[\mu_h + (e_0 + \varepsilon I)\big(1 - \rho/(\rho + \mu_E)\big)\big]H = 0$, and $1 - \rho/(\rho + \mu_E) = \theta$, which gives (a). (b) Setting $I = 0$ in (a) gives $\widetilde{H}_0$. The only infected compartment is still $I$, and the argument of Theorem 1 with $H_0$ replaced by $\widetilde{H}_0$ gives $\tilde{\mathcal{R}}_0$. At the disease-free equilibrium the row of the Jacobian for $I$ has the single non-zero entry $\beta - \gamma - \kappa\widetilde{H}_0$, on the diagonal, so this is an eigenvalue; it is negative if $\tilde{\mathcal{R}}_0 < 1$ and positive if $\tilde{\mathcal{R}}_0 > 1$. The other three eigenvalues are those of the matrix of the linear workforce system in $(T, H, E)$,

$$A = \begin{pmatrix} -k_t & 0 & 0 \\ \sigma & -(\mu_h + e_0) & \rho \\ e_t & e_0 & -(\rho + \mu_E) \end{pmatrix}. \tag{42}$$

The off-diagonal entries of $A$ are non-negative and its column sums are $-\mu_t$, $-\mu_h$ and $-\mu_E$, all negative, so by the Gershgorin theorem applied to the columns every eigenvalue of $A$ has negative real part. (c) At an equilibrium the treatment term in the equation for $I$ is $\kappa HI/(1 + bI) = \kappa\tilde{\pi} I/\big((\tilde{m} + \tilde{\varepsilon} I)(1 + bI)\big)$, which is the function $G$ of (17) with the replaced parameters; Lemma 2 and Theorems 3 and 4 use only the properties of $h$, and $\tilde{m}$ increases with $e_0$ as $m$ does. (d) If $\rho > 0$, then $\theta < 1$, so $\tilde{m} \leq m$, and $\tilde{\pi} > \pi$ because $e_t > 0$; hence $\widetilde{H}_0 > H_0$ and $\tilde{\mathcal{R}}_0 < \mathcal{R}_0$. Finally $\tilde{\varepsilon}/\tilde{m}_c = \theta\varepsilon(\beta - \gamma)/(\kappa\tilde{\pi}) < \varepsilon(\beta - \gamma)/(\kappa\pi) = \varepsilon/m_c$ when $\varepsilon > 0$. ■

Theorem 8 covers the equilibria and the threshold. Theorems 5 and 6 concern the planar limit system (3); with return migration, $E$ feeds back into $H$ and the limit system is three-dimensional, so the Dulac argument does not apply, and the stability of the endemic equilibria and global convergence have not been established for the extended model.

Return migration therefore acts in two ways: it raises the disease-free workforce, which lowers the reproduction number, and it weakens the burnout feedback by the factor $\theta$, which lowers the index. For an illustration I take $\mu_E = 0.05$ per year, so that emigrants remain possible returners for 20 years on average, $e_0 = 0.08$, $b = 0$ and the other values in Table 1. Without return ($\rho = 0$), $\tilde{\mathcal{R}}_0 = 0.936$ and $\widetilde{\Psi}_c = 2.13$, and there are two endemic equilibria with prevalences 0.060 and 0.323, as in Figure 4. With $\rho = 0.02$ per year,

$\tilde{\mathcal{R}}_0 = 0.781$ and $\tilde{\Psi}_c = 1.48$; with $\rho = 0.05$ per year, $\tilde{\mathcal{R}}_0 = 0.655$ and $\tilde{\Psi}_c = 1.02$. In both cases the bifurcation is still backward, but the fold has moved past $e_0 = 0.08$, so no endemic equilibrium exists there and the bistability of Figure 4 disappears. The values of $\rho$ and $\mu_E$ are assumptions, not estimates.

### 3.9 Discussion

The analysis has three implications for the interpretation of workforce policy. First, a health system can lose control of an infection without any change in transmission, simply because its workforce shrinks. Corollary 1 gives the critical workforce $H_c$ and the corresponding critical values of emigration and training intake. Second, when burnout makes emigration sensitive to the disease burden and $\Psi_c > 1$, keeping $\mathcal{R}_0$ below one is not enough: for $e_0^{sn} < e_0 < e_0^c$ a large outbreak can push the system to a stable endemic state. Third, the loss of control is hard to reverse. Once the endemic state is reached, emigration must be reduced to $e_0^{sn}$, or training raised to $\Lambda_{sn}$, rather than merely returned to the critical value. Measures that reduce burnout, which lower $\varepsilon$, leave $\mathcal{R}_0$ unchanged but shrink the interval of bistability and remove it when $\Psi_c \leq 1$. By (13), at baseline a given percentage change in the training intake has a larger effect on $\mathcal{R}_0$ than the same percentage change in the baseline emigration rate.

The relation to earlier work should be stated plainly. If the workforce is at its quasi-equilibrium $H = \pi/(m + \varepsilon I)$ and $b = 0$, the treatment term becomes $\kappa\pi I/(m + \varepsilon I)$, which has the saturating form of the treatment functions studied by Zhang and Liu [25]. The equilibrium structure of my model is therefore related to theirs. What the coupled model adds is the origin of the saturation and its expression in workforce parameters: the saturation constant is $\varepsilon/m$, so it is set by the burnout response and the exit rate, and the thresholds $e_0^c$, $e_0^{sn}$, $\Lambda_c$ and $\Lambda_{sn}$ are stated in quantities that a health ministry can influence. The model also keeps the slow time scale of the workforce, which produces the long transient in Figure 4(a). Backward bifurcation has several known causes in epidemic models [4, 6, 8]; the feedback studied here works through the capacity of the health system rather than through the biology of the infection.

Table 3 compares the present model with the fixed-capacity models discussed in the introduction. In each of those models the treatment term depends on prevalence through a fixed capacity, a fixed saturation constant or a fixed number of beds, whereas here the capacity is the state variable $H$, and its dependence on prevalence comes from emigration. Without saturation ($b = 0$) the present model has a backward bifurcation exactly when $\Psi_c = \varepsilon I_{\max}/m_c > 1$, a condition stated entirely in workforce parameters.

**Table 3.** Treatment or recovery terms and reported bifurcations in models with limited treatment, compared with the present model.

| Model | Treatment or recovery term | What limits treatment | Bifurcations reported |
|---|---|---|---|
| Wang and Ruan [20] | constant removal $r$ for $I > 0$ | fixed removal rate | Bogdanov–Takens, Hopf, homoclinic |
| Wang [19] | $rI$ for $I \leq I_0$, $rI_0$ for $I > I_0$ | fixed capacity $I_0$ | backward |
| Zhang and Liu [25] | $rI/(1 + \alpha I)$ | fixed saturation constant $\alpha$ | backward |
| Zhou and Fan [27] | saturated treatment | fixed medical resources | Hopf, Bogdanov–Takens |
| Shan and Zhu [16] | recovery rate $\mu_0 + (\mu_1 - \mu_0)b/(I + b)$ | fixed number of beds $b$ | backward, saddle-node, Hopf, Bogdanov–Takens |
| Hsiao and Juang [10] | capacity of Wang [19] with behavioural change | fixed capacity set by policy | degenerate Hopf, saddle-node of limit cycles |
| This paper | $\kappa HI/(1 + bI)$ with $H$ from (1) | workforce $H$, reduced by burnout-driven emigration | backward (with or without saturation), closed-form hysteresis |

The numerical results rest on assumed parameter values, and this is the main limitation of the study. Four parameters decide the thresholds and would have to be estimated before the model could be applied to a real health system. The baseline emigration rate $e_0$ is the annual fraction of practising workers who emigrate when the disease burden is low; it could be estimated from annual counts of departures, for example from the registers of destination countries such as that of the Nursing and Midwifery Council [13], divided by the size of the home register. The burnout sensitivity $\varepsilon$ is the increase in that rate per unit of prevalence; estimating it requires emigration rates together with measures of disease burden or workload over several years, or across states or facilities, so that the effect of workload can be separated from other causes of emigration. The

treatment rate per health worker $\kappa$ could be estimated from facility records of the number of cases treated per worker per year when caseloads are light, and the saturation constant $b$ from how the time to treatment lengthens as the caseload rises. Surveys such as [1, 2, 3, 14] show that burnout and the intention to emigrate are linked, but they measure intention rather than departures and so do not give $\varepsilon$ directly.

The model has further limitations. It neglects infection of health workers, its infection is of SIS type and so stands for a treatable disease without lasting immunity, and the emigration rate is assumed to rise linearly with prevalence. Return migration is treated only at the level of equilibria and the threshold (Theorem 8).

## 4 Conclusion

I have coupled a treatable SIS infection to a health workforce that is trained, practises and emigrates, with emigration that rises with the disease burden. The basic reproduction number depends on the workforce through its disease-free level, which yields explicit critical values of the workforce, the baseline emigration rate and the training intake. Burnout-driven emigration alone can make the bifurcation backward; the index $\Psi_c = I_{\max}(b + \varepsilon/m_c)$ decides the direction, and centre manifold theory gives the same criterion. Without treatment saturation the fold, the hysteresis width and the jump in prevalence are explicit, and under the condition $b(\beta - \gamma) \leq \beta$ every solution converges to an equilibrium. The simulations show that a system that loses control of an infection through emigration needs a larger correction than the one that caused the loss. Allowing emigrants to return raises the disease-free workforce and weakens the burnout feedback, so it lowers both the reproduction number and the index. All parameter values in this study are illustrative assumptions; applying the model to Nigeria or to any other health system requires estimates of $e_0$, $\varepsilon$, $\kappa$ and $b$ from data on departures, workload and treatment, as set out in Section 3.9.

## Acknowledgements

The author has no acknowledgements to make.

## Declarations

**Funding.** This study received no funding.

**Competing interests.** The author declares no competing interests.

**Ethics approval and consent.** Not applicable. The study uses no human or animal data.

**Data and code availability.** No new data were generated. All parameter values used in this study are listed in Table 1, and all the symbolic computations are available from the author on request.

**Author contributions.** T. A. Shamaki is the sole author and carried out the conceptualization, analysis, computation and writing.

**Use of AI tools.** The author declares nonuse of an AI tool/assistant.

## References

[1] M.A. Adeniyi, O. Efuntoye, G. Popoola, et al., Profile and determinants of intention to migrate by early career doctors in Nigeria: A report from CHARTING study. International Journal of Health Planning and Management, 37(3), 2022, 1512–1525. https://doi.org/10.1002/hpm.3422

[2] D.O. Ajayi, C. Tanova, S.W. Bayighomog, A.S. Akinwande, Decent work conditions and Nigerian nurse emigration: The role of burnout and commitment. Acta Psychologica, 259, 2025, 105294. https://doi.org/10.1016/j.actpsy.2025.105294

[3] O.A. Badru, T.A. Alabi, S.S. Okerinde, M.A. Kabir, A. Abdulrazaq, O.A. Adeagbo, F.A. Badru, Investigating the emigration intention of health care workers: A cross-sectional study. Nursing Open, 11(5), 2024. https://doi.org/10.1002/nop2.2170

[4] F. Brauer, Backward bifurcations in simple vaccination models. Journal of Mathematical Analysis and Applications, 298(2), 2004, 418–431. https://doi.org/10.1016/j.jmaa.2004.05.045

[5] C. Castillo-Chavez, B. Song, Dynamical models of tuberculosis and their applications. Mathematical Biosciences and Engineering, 1, 2004, 361–404. https://doi.org/10.3934/mbe.2004.1.361

[6] J. Dushoff, W. Huang, C. Castillo-Chavez, Backwards bifurcations and catastrophe in simple models of fatal diseases. Journal of Mathematical Biology, 36(3), 1998, 227–248. https://doi.org/10.1007/s002850050099

[7] N. Gozalpour, E. Badfar, A. Nikoofard, Transmission dynamics of novel coronavirus SARS-CoV-2 among healthcare workers, a case study in Iran. Nonlinear Dynamics, 105(4), 2021, 3749–3761. https://doi.org/10.1007/s11071-021-06778-5

[8] A.B. Gumel, Causes of backward bifurcations in some epidemiological models. Journal of Mathematical Analysis and Applications, 395(1), 2012, 355–365. https://doi.org/10.1016/j.jmaa.2012.04.077

[9] H.W. Hethcote, The mathematics of infectious diseases. SIAM Review, 42(4), 2000, 599–653. https://doi.org/10.1137/S0036144500371907

[10] A.-T. Hsiao, J. Juang, The effect of limited medical resource, socio-economic processes and their time scales on epidemic models. Journal of Nonlinear Science, 36(1), 2026, 17. https://doi.org/10.1007/s00332-025-10231-x

[11] S. Marino, I.B. Hogue, C.J. Ray, D.E. Kirschner, A methodology for performing global uncertainty and sensitivity analysis in systems biology. Journal of Theoretical Biology, 254(1), 2008, 178–196. https://doi.org/10.1016/j.jtbi.2008.04.011

[12] K. Mischaikow, H. Smith, H.R. Thieme, Asymptotically autonomous semiflows: Chain recurrence and Lyapunov functions. Transactions of the American Mathematical Society, 347(5), 1995, 1669–1685. https://doi.org/10.1090/S0002-9947-1995-1290727-7

[13] Nursing and Midwifery Council, The NMC register: 1 April 2021 – 31 March 2022. Nursing and Midwifery Council, London, 2022. https://www.nmc.org.uk/globalassets/sitedocuments/data-reports/march-2022/nmc-register-march-2022.pdf (accessed 18 October 2026).

[14] C.K. Onah, B.N. Azuogu, C.N. Ochie, C.O. Akpa, K.C. Okeke, A.O. Okpunwa, H.M. Bello, G.O. Ugwu, Physician emigration from Nigeria and the associated factors: The implications to safeguarding the Nigeria health system. Human Resources for Health, 20, 2022, 85. https://doi.org/10.1186/s12960-022-00788-z

[15] L. Perko, Differential Equations and Dynamical Systems, 3rd ed., Texts in Applied Mathematics 7. Springer, New York, 2001. https://doi.org/10.1007/978-1-4613-0003-8

[16] C. Shan, H. Zhu, Bifurcations and complex dynamics of an SIR model with the impact of the number of hospital beds. Journal of Differential Equations, 257(5), 2014, 1662–1688. https://doi.org/10.1016/j.jde.2014.05.030

[17] H.R. Thieme, Convergence results and a Poincaré-Bendixson trichotomy for asymptotically autonomous differential equations. Journal of Mathematical Biology, 30(7), 1992, 755–763. https://doi.org/10.1007/BF00173267

[18] P. van den Driessche, J. Watmough, Reproduction numbers and sub-threshold endemic equilibria for compartmental models of disease transmission. Mathematical Biosciences, 180(1–2), 2002, 29–48. https://doi.org/10.1016/S0025-5564(02)00108-6

[19] W. Wang, Backward bifurcation of an epidemic model with treatment. Mathematical Biosciences, 201(1–2), 2006, 58–71. https://doi.org/10.1016/j.mbs.2005.12.022

[20] W. Wang, S. Ruan, Bifurcations in an epidemic model with constant removal rate of the infectives. Journal of Mathematical Analysis and Applications, 291(2), 2004, 775–793. https://doi.org/10.1016/j.jmaa.2003.11.043

[21] WHO Regional Office for Africa, WHO, UK Government, supports Nigeria in developing a strategic approach to managing health workforce migration. News release, 6 September 2024. https://afro.who.int/pt/node/19864 (accessed 18 October 2026).

[22] World Health Organization, Global strategy on human resources for health: Workforce 2030. World Health Organization, Geneva, 2016. ISBN 978 92 4 151113 1. https://www.who.int/publications/i/item/9789241511131

[23] World Health Organization, WHO health workforce support and safeguards list 2023. World Health Organization, Geneva, 2023. ISBN 978-92-4-006978-7. https://www.who.int/publications/i/item/9789240069787

[24] World Health Organization, Medical doctors (per 10 000 population), Global Health Observatory indicator HWF_0001, Nigeria, 2026. https://ghoapi.azureedge.net/api/HWF_0001 (accessed 18 October 2026).

[25] X. Zhang, X. Liu, Backward bifurcation of an epidemic model with saturated treatment function. Journal of Mathematical Analysis and Applications, 348(1), 2008, 433–443. https://doi.org/10.1016/j.jmaa.2008.07.042

[26] X.-Q. Zhao, Dynamical Systems in Population Biology. CMS Books in Mathematics. Springer, Cham, 2017. https://doi.org/10.1007/978-3-319-56433-3

[27] L. Zhou, M. Fan, Dynamics of an SIR epidemic model with limited medical resources revisited. Nonlinear Analysis: Real World Applications, 13(1), 2012, 312–324. https://doi.org/10.1016/j.nonrwa.2011.07.036